



ELSEVIER

Physics of the Earth and Planetary Interiors 119 (2000) 269–283

PHYSICS
OF THE EARTH
AND PLANETARY
INTERIORS

www.elsevier.com/locate/pepi

Electric field polarization around Ioannina VAN station, Greece, inferred from a resistivity mapping

Wataru Kanda^{a,*}, Makoto Uyeshima^b, John Makris^c, Yoshiaki Orihara^a,
Hideaki Hase^{d,1}, Toshiyasu Nagao^d, Seiya Uyeda^a

^a *The Institute of Physical and Chemical Research (RIKEN), c/o Earthquake Prediction Research Center, Tokai University, Orido 3-20-1, Shimizu 424-8610, Japan*

^b *Earthquake Research Institute, University of Tokyo, Yayoi 1-1-1, Bunkyo-ku, Tokyo 113-0032, Japan*

^c *Solid Earth Physics Institute, University of Athens, Zografos, Athens, 157-84, Greece*

^d *Earthquake Prediction Research Center, Tokai University, Orido 3-20-1, Shimizu 424-8610, Japan*

Received 3 February 1999; accepted 15 December 1999

Abstract

In the summer of 1997, we made a bipole–dipole mapping survey around Ioannina station of VAN (Varotsos, Alexopoulos, and Nomicos), where detection of the pre-seismic electric signal (SES) has been repeatedly reported. Since we had found the characteristic directional properties of the electric field in the previous study, the present study was aimed to examine it by investigating the shallow electric structure around the station. The apparent resistivity tensor was derived from two sets of measured voltages at each receiver position. From a rough sketch of the resistivity tensor distribution, we found that the electric field was enhanced along the direction parallel to the trend of the basin at receivers located in the conductive basin, and perpendicular to it at receivers in the resistive mountainside. Conductance distribution models with thin plates were constructed by using the measured voltages. The results showed that the VAN station is located on the resistive portion near the contact between the conductive and the resistive part. Furthermore, we simulated the apparent resistivity tensor near the VAN station on the inferred conductance distribution model. Although the directional property similar to those of magnetotelluric (MT) and lightning electric field was not reproduced there, we found that the electric field polarization is affected by heterogeneous structure not only around receivers but also around the source. © 2000 Elsevier Science B.V. All rights reserved.

Keywords: Bipole–dipole mapping; Electrical structure; Conductance; SES; Greece

1. Introduction

In Greece, electrical potential difference measurements with a set of short and long dipoles on the ground have been applied to the earthquake prediction since early 1980s (Varotsos and Alexopoulos, 1984a,b, 1987). This VAN method defines measured

* Corresponding author. Sakurajima Volcano Research Center, Disaster Prevention Research Institute, Kyoto University, Sakurajima, Kagoshima 891-1419, Japan. Fax: +81-99-293-4024.

E-mail address: kanda@svo.dpri.kyoto-u.ac.jp (W. Kanda).

¹ Current address: Aso Volcanological Laboratory, Institute for Geothermal Sciences, Graduate School of Science, Kyoto University, Choyo, Aso, Kumamoto 869-1404, Japan.

anomalous voltages that satisfy some conditions as the seismic electric signal (SES) and makes a prediction based on the relationship between anomalous voltages and earthquake which was empirically found in the past decades. However, physical basis of the SES has not been completely clarified despite many efforts (Varotsos et al., 1996c, 1998).

To examine the physical properties of the SES, our group has carried out a series of field surveys around Ioannina station, northwestern Greece, where the SES has been most frequently observed. Results of the previous surveys are summarized as follows.

(1) Despite that the magnetic field of the earth's exterior origin fluctuated in random direction, the induced electric field varied only in the nearly N68°E direction. The same polarized direction for the magnetotelluric (MT) field variation was also reported by Varotsos et al. (1996a,b). The electric field variation of the lightning origin was also bound to the same direction, although it deviated more from that direction as the lightning came nearer to the station. On the other hand, the directions of the SES field variations were more scattered (Uyeshima et al., 1998).

(2) When the electric current was injected to the ground at several kilometers away from the station, the direction of the measured voltage variation seemed to follow the same property as that of the external magnetic field origin (Ogawa et al., 1996).

These results were considered to suggest that the origin of the SES is located within a few kilometers from the Ioannina station. Hereafter, the term "origin" will be used for the outlet of the SES if it is generated at earthquake source as the VAN method claims (e.g., Varotsos and Alexopoulos, 1986). However, the above results could not be strongly asserted. The first was derived from the electromagnetic field measurement at only one receiver position in the Ioannina station. The second result had low reliability because the intensity of the transmitted current moment was too small (~ 0.5 [A] \times 100 [m]).

Since the inferred electrical resistivity structure from the MT survey beneath a few kilometers depth was almost two dimensional (2-D) and the polarization of the telluric field variation was concordant with that of the regional 2-D strike after Groom and Bailey (1989) (G–B) decomposition analysis (Hori et al., 1996; Makris et al., 1997), the polarized MT

field variation at the Ioannina station may be caused by the resistivity contrast of the regional strike. However, the polarized direction observed at another electric field station, which was installed by the French group about 4.5 km northwest from the VAN station, was completely different from that observed at the VAN station for the same MT signal (Gruszko et al., 1996). Although they claimed that the proximity and the orientation of the source caused the difference, the local heterogeneity should affect the electric field polarization as well. The G–B decomposition clearly indicated the existence of geological noise due to near-surface heterogeneity (Hori et al., 1996; Makris et al., 1997). Recently, the VAN group proposed a model in which the observed SES was efficiently amplified due to the end effect of a conductive channel (Varotsos et al., 1996c, 1998). Taking these results into consideration, we conducted a bipole–dipole survey around Ioannina station under the cooperation with the VAN group to examine the heterogeneity or directional property of the shallow electrical structure.

2. Experiment

The VAN station in Ioannina is located inside the Greek army camp several kilometers away from the Ioannina city center. We installed two electric current bipoles in two orthogonal directions northwest of the VAN station (Fig. 1). Bipole length was about 480 m in the NE–SW direction and about 380 m in the NW–SE direction. Both ends of each bipole were composed of multiple steel rods. The VIP 3000 system (IRIS INSTRUMENTS, France) was used as a current transmitter that was placed at the intersection of two bipoles. The maximum output power of the VIP 3000 is 3 kW, affording to transmit the maximum output current of 5 A. Contact resistance of each bipole was 200 to 400 Ω , so that stably transmitted current with these poles was about 2.0 A (NE–SW bipole) and 3.0 A (NW–SE bipole).

Receivers were placed from a few hundred meters to several kilometers away from the source bipoles as shown by black dots in Fig. 1. Orthogonal two horizontal components of the electric field were measured for each current bipole direction at 30 receiver positions. The length of receiving dipole

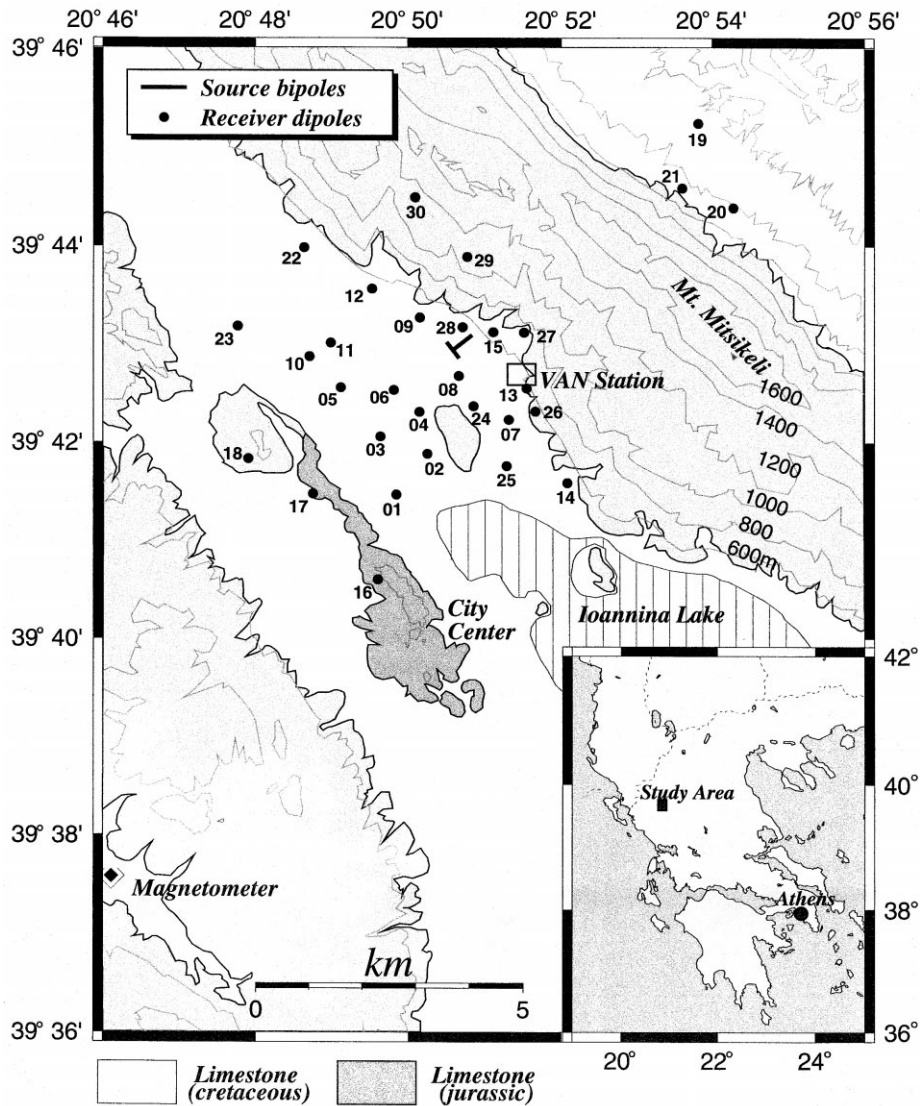


Fig. 1. Configuration of a bipole–dipole mapping survey carried out in the summer of 1997. A simplified geology map (distribution of Mesozoic limestone outcrops) is shown on the background.

was about 45 m, although it was reduced to about 30 m in a few receiver positions due to geographical restriction. The transmitted current was square wave of a 10-s period, which consisted of a 4-s transmitting interval and a 1-s stopping interval for each sign. The electric current was transmitted at least for 20 min for each bipole direction. We used a hand-made Cu–CuSO₄ electrode as receiving probe. The

data were stored in 12 bit binary format with 10 Hz sampling rate by a data-logger DATAMARK LS3300ptV (Hakusan, Tokyo). The range for the electric records was ± 2 V.

In the previous experiment with the controlled source, the measured voltages were unclear because the telluric current induced by the external geomagnetic field was too large compared to the artificial

signal (Ogawa et al., 1996). In order to eliminate the telluric effects, we also installed a fluxgate-type magnetometer about 10 km away from the source. However, we did not have to use the magnetic field data at all because the geomagnetic field was quiet during the experiment period.

3. Apparent resistivity

In Fig. 2, we show four examples of the stacked data. IOA13 is the nearest receiver to the VAN station. Reliability of the stacked voltages can be evaluated by their standard deviation. At IOA10 and IOA13, the square waveform due to the transmitted current can be clearly recognized after stacking. The waveform measured at IOA21 is considered to represent a significant signal. In the stacked data at IOA16, we cannot detect any clear square waveform because the site is close to the city center and the raw data are not of good quality. Since receivers were not exactly synchronized with the transmitted current timing, we used a simple correlation between the observed voltages and the presumed square waveform of the transmitter, which is a similar methodology used by Park and Fitterman (1990). At some receiver positions such as IOA13 in Fig. 2, transient signals were included in the data, so that we only used the portion of the data without such transient signals to obtain the observed voltage. The stacked data were averaged again along the time axis shown in Fig. 2: the difference between the averaged value for 3 s (1.6–4.5 s in the figure) and the averaged value for 0.6 s (0.3–0.8 s) was defined as the measured voltage at a site in consideration of inaccurate synchronization between the transmitter and the receiver. Then two components of the electric field were calculated by dividing the voltage by the separation of probing electrodes.

Using the theoretical expression by Bibby (1986), the apparent resistivity tensor was computed from the measured electric field and the current density calculated from the source–receiver configuration assuming the uniform earth. Since we had two sets of the electric field data, we were able to determine

all components of the apparent resistivity tensor. That is, on the appropriate x – y coordinates,

$$\begin{pmatrix} E_{x(\text{NE-SW})} & E_{x(\text{SE-NW})} \\ E_{y(\text{NE-SW})} & E_{y(\text{SE-NW})} \end{pmatrix} = \begin{pmatrix} \rho_{xx} & \rho_{xy} \\ \rho_{yx} & \rho_{yy} \end{pmatrix} \begin{pmatrix} I_{x(\text{NE-SW})} & I_{x(\text{SE-NW})} \\ I_{y(\text{NE-SW})} & I_{y(\text{SE-NW})} \end{pmatrix} \quad (1)$$

where E , I , and ρ denote the measured electric field, the current density, and the apparent resistivity, respectively. It is considered that the apparent resistivity reflects the averaged resistivity down to the depth comparable to a fraction of the source–receiver separation.

In Fig. 3(a), we show the distribution of the apparent resistivity that is defined by the determinant of the resistivity tensor calculated from Eq. (1). The error distribution of the resistivity that was estimated from the standard deviation of the stacked data is also shown as percentage in the background. The darker color indicates the greater error. The apparent resistivity varies from about 50 to 600 Ω m in the study area. As a general tendency, the area corresponding to the alluvium basin shows low resistivity of about several tens to a hundred ohm meters. On the other hand, areas corresponding to the mountain of the Mesozoic limestone show high resistivity of several hundreds ohm meters. However, the apparent resistivity distribution is not always exactly coincident with the geological features. A little difference from this tendency can be seen at some receivers: in the basin around IOA05 towards IOA23 the resistivity increases to more than 200 Ω m, while about 100 Ω m was observed at IOA18 and at IOA27 on the mountainside. At three remote receivers in the north-eastern foot of the Mitsikeli mountains (see Fig. 1), low resistivity of several tens ohm meters was observed, although the reliability is rather low. Nearby, the VAN station, around IOA13, the area shows high resistivity of 300 to 400 Ω m. The resistivity appears to be reduced towards east of IOA13, but it is likely to be resistive because we have no receivers in that mountain area.

In Fig. 3(b), the locus of each tensor is traced when we rotate the resistivity tensor defined by Eq. (1) by 360°. These loci are equivalent with those of the electric field if a unit current density vector is rotated. The direction of the major axis of ellipses is

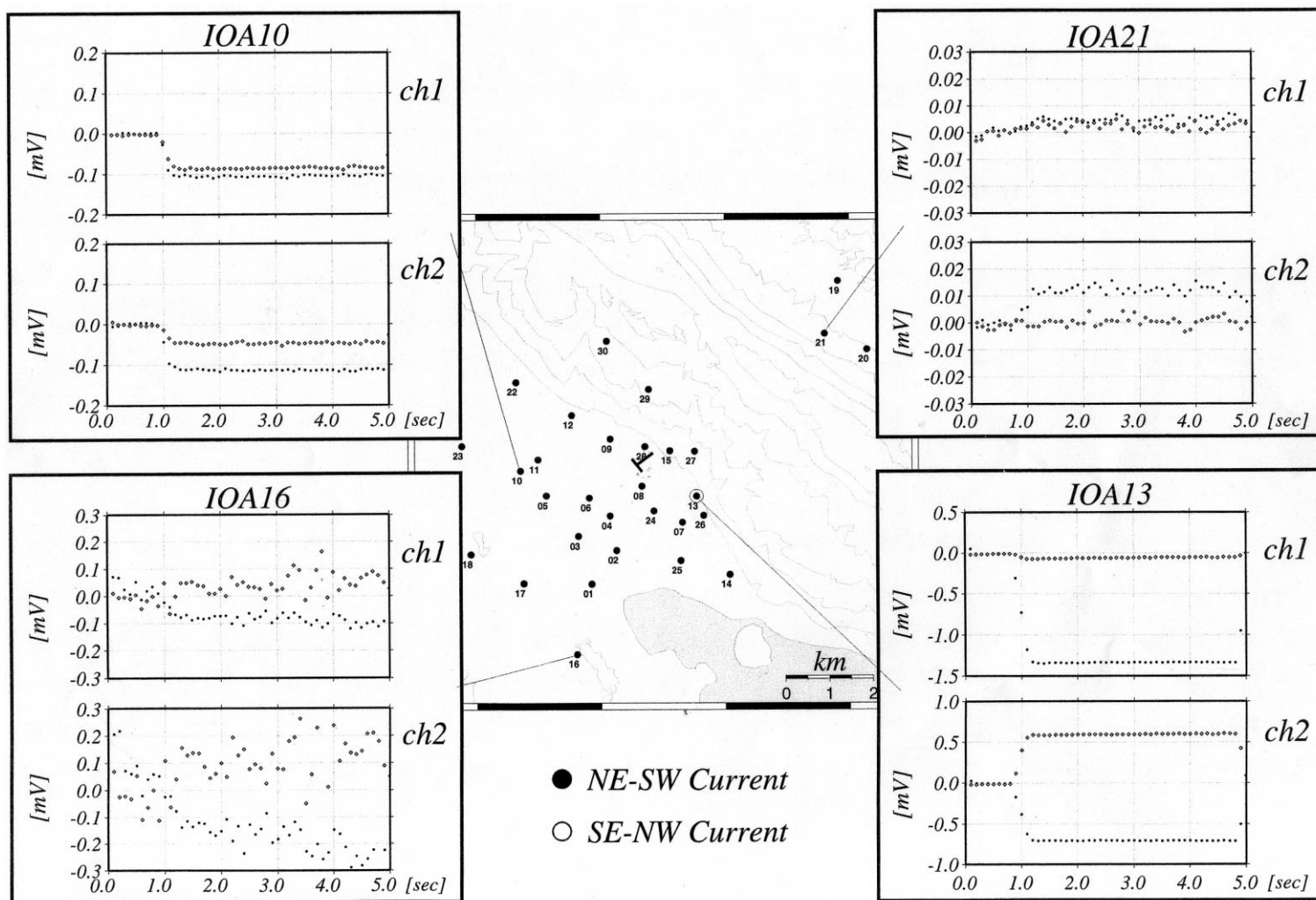


Fig. 2. Stacked data obtained at IOA10, IOA13, IOA16, and IOA21 for current injections into two different bipoles. The horizontal axis is time for 5 s, which is composed of 1 s of no current and 4 s of current transmission.

equal to the direction that makes the largest electric fields. As a rough trend, the major axis oriented parallel to the basin at receiver positions located in the basin, and orthogonal to the alluvium–limestone contact at receivers located on the foot of mountains. The direction of the major axis at IOA13 is about N57°E/N237°E, which is consistent with the polarized direction (N68°E/N248°E) of the telluric field induced by the external magnetic disturbances.

4. Conductance map

Although the apparent resistivity distribution may express the rough trend of the subsurface structure, it is derived under the assumption of a uniform earth. To understand the lateral heterogeneity around Ioan-

nina station, we modeled it by thin plates because the measured electric field data were considered to be affected by near-surface heterogeneity. As shown in the upper panel of Fig. 4, a surface with infinitesimal thickness h just under the ground is divided into $M \times N$ plates, each with constant conductance. For a plate conductivity of $\sigma_{i,j}$, the resistance of the plate can be expressed as:

$$R_{i,j,x} = \frac{1}{\sigma_{i,j}} \frac{a_i}{b_j h} = \frac{1}{S_{i,j}} \frac{a_i}{b_j} \quad (i = 1-M) \quad (2)$$

$$R_{i,j,y} = \frac{1}{\sigma_{i,j}} \frac{b_j}{a_i h} = \frac{1}{S_{i,j}} \frac{b_j}{a_i} \quad (j = 1-N) \quad (3)$$

where a_i , b_j , and $S_{i,j} = \sigma_{i,j} h$ are the length in x -, y -direction, and the conductance of the plate. An

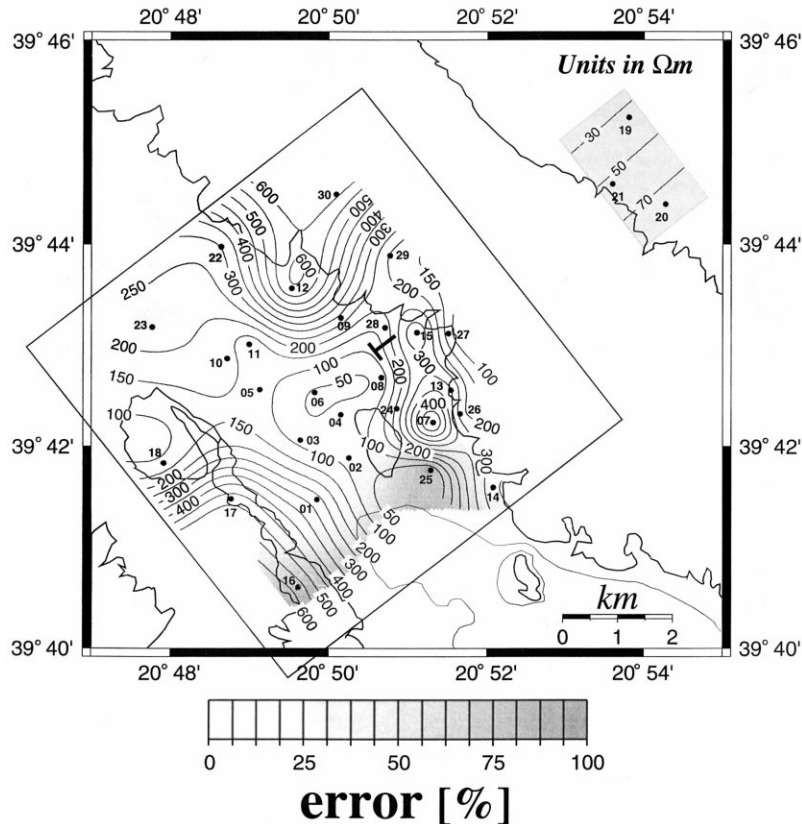


Fig. 3. (a) Apparent resistivity distribution represented by the determinant of the resistivity tensor. In the background, the apparent resistivity error distribution estimated from the standard deviation of the measured voltage is also shown as percentage. The solid line represents the simplified geological boundary (Fig. 1). Inclined square shows the computation area assigned in the later modeling. (b) Elliptical representation of the apparent resistivity tensors derived from the bipole–dipole mapping.

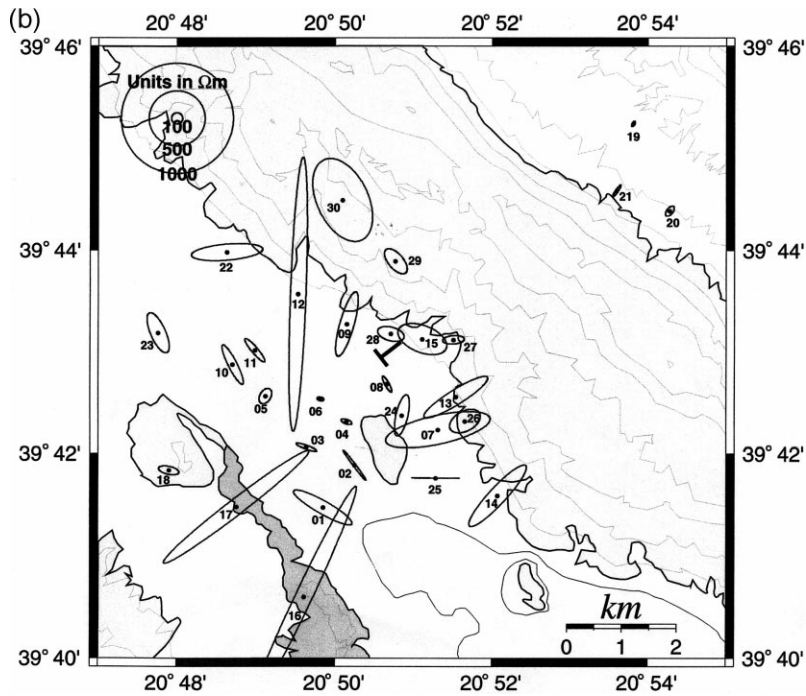


Fig. 3 (continued).

ensemble of plates can be replaced with an equivalent grid of resistance (Madden, 1972; Madden and Swift, 1969), which enables us to calculate the potential distribution inside the calculation domain with an appropriate boundary condition. The modified mixed boundary condition used by Zhang et al. (1995) was applied on the domain boundary. Consequently, we can get the electric potential at all the nodes (center of the plate). Since the measured data were two components of the electric field, we interpolated the potential values by using the 2-D natural spline and then computed the electric field at each receiver position.

Conductance distribution was estimated by inversion. Inversion parameter is the conductance $S_{i,j}$ shown in the above equations. Neither the thickness h nor the conductivity $\sigma_{i,j}$ is specified. We used a weighted least square scheme with a smoothing constraint, which is based on the maximization of a Bayesian likelihood (e.g., Uchida, 1993). The absolute values of the electric field components were assigned as the observed data, and two sets of the observed data for different bipole sources were used

together to estimate the plate conductance. The data obtained in the northeastern foot of the Mitsikeli mountains (IOA19, 20, 21) were not used in the inversion because those three receivers were isolated from others. The computation area for the electric potential and current was $7680 \times 7680 \text{ m}^2$, which was inclined at 52° from north to east (see Fig. 3(a)). We divided this area into 80×80 square plates of $96 \times 96 \text{ m}^2$. The same conductance value was assigned to a block of 5×5 plates, so that the unknown conductance for 16×16 blocks was estimated by the inversion.

In Fig. 5, a result of a checker board test is shown. The model shown by Fig. 5(b) was derived from the synthetic data calculated from the model shown by Fig. 5(a) in which the conductance of 0.1 or 10 S was given alternately to the units each consisting of 4×4 blocks. Since the smoothly changed model was estimated by the inversion, no sharp boundary can be obtained. Around the center of the computation area, the degree of reproduction is high because several receivers are included in the group of blocks. On the other hand, for some sec-

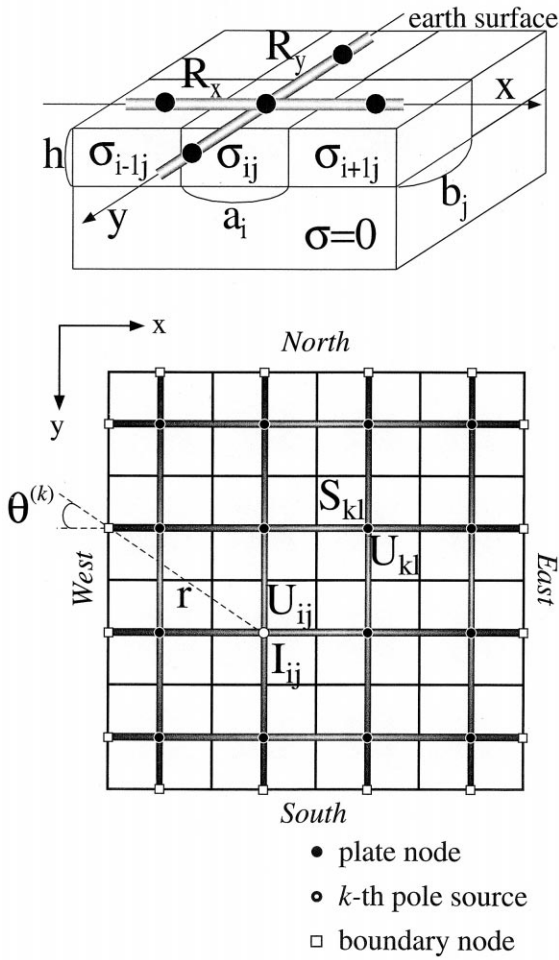
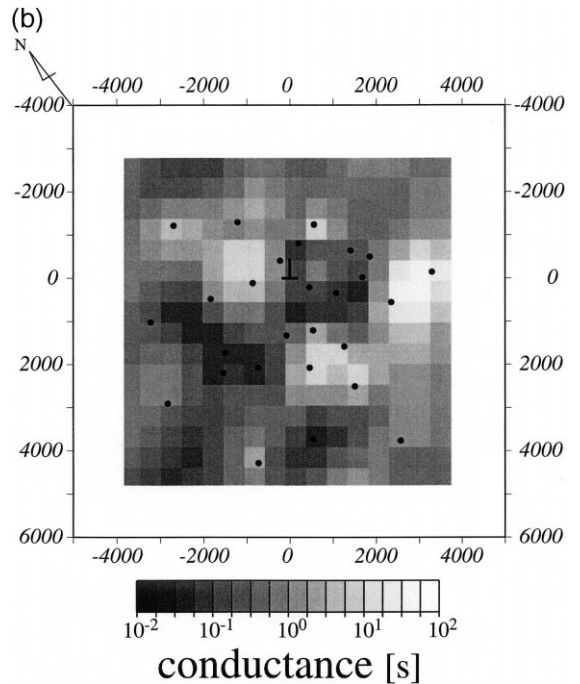
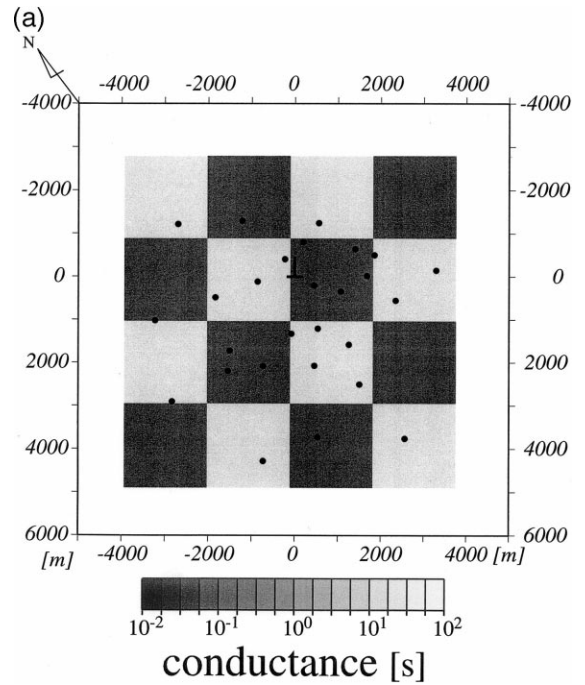


Fig. 4. Model calculation by infinitely thin plates. Upper panel: the ensemble of the thin plates at the surface with conductivity $\sigma_{i,j}$, which can be replaced by the resistance network. R_x and R_y represent the resistance in x - and y -direction, respectively and are represented by Eq. (3). Lower panel: a plan view of the resistance network. Each resistance is connected at the node located in the center of each plate, which is referred as ‘‘plate node’’. In the domain boundary, the resistance terminated at the ‘‘boundary node’’.

tions where only one receiver is located, conductance values are well reproduced only near the respective receiver. Furthermore, it is sometimes the case that

Fig. 5. (a) An original model for the checker board test. The presented area is inclined at 52° from the north to the east. Black dots depict the receiver positions and thin lines show bipole sources. (b) Result of the checker board test. The synthetic data calculated from the model shown in (a) were inverted.



conductance values are not reproduced at all for the sections with no receiver.

Fig. 6(a) shows the best-fit conductance distribution model around Ioannina station inferred from the bipole–dipole survey in the summer of 1997. In Fig.

6(b), we compare the observed apparent resistivity ellipses (Fig. 3(b)) with the synthetic ones when the best-fit conductance distribution model (Fig. 6(a)) was given. Spatial distribution of the inversion parameter uncertainty is also shown as percentage in

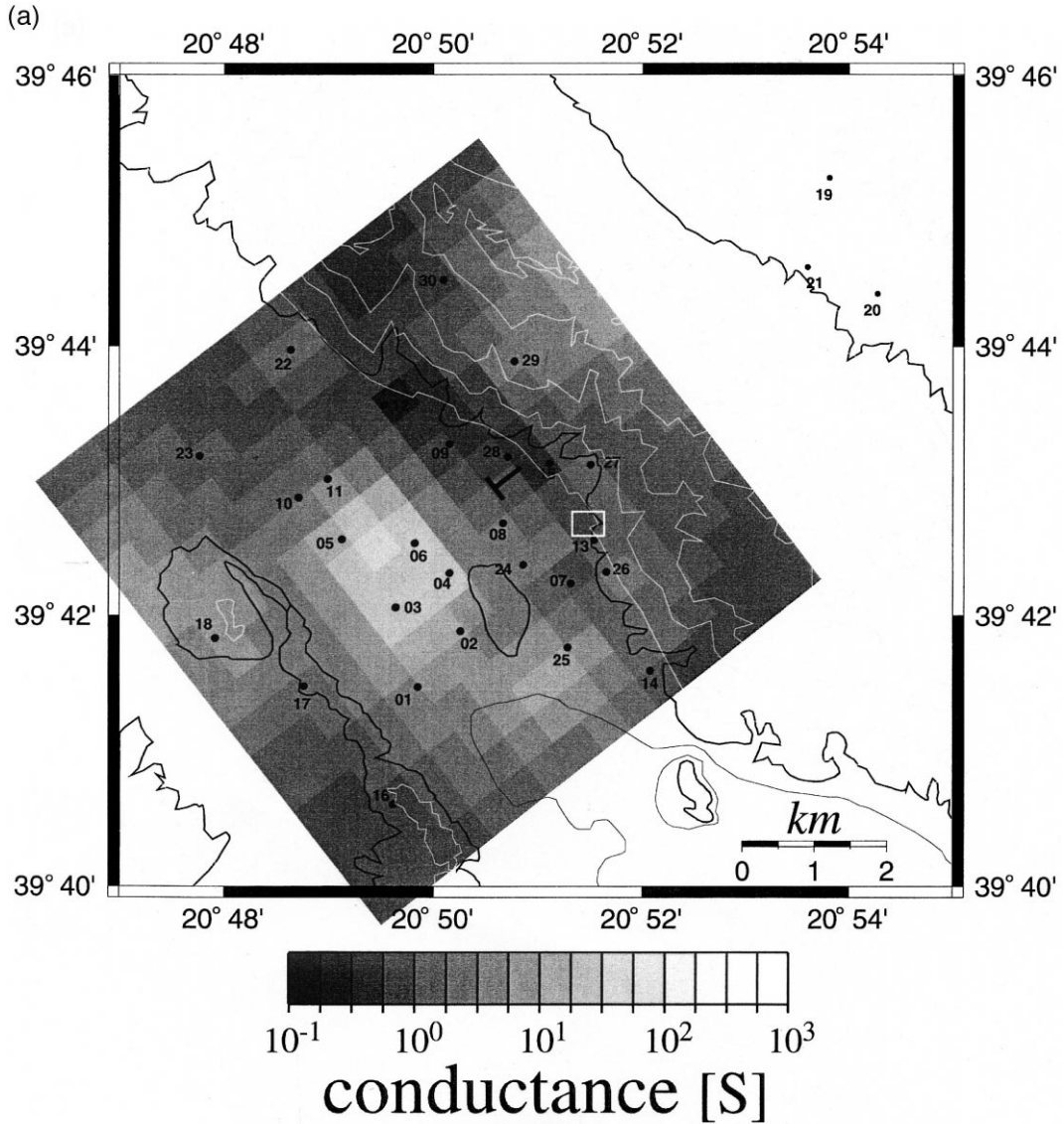


Fig. 6. (a) The best-fit conductance distribution model. The presented region is inclined at 52° from the north to the east. Black dots depict the receiver positions and bipole sources are shown by thin lines. The simplified geological boundaries (Fig. 1) are also drawn by solid lines. The VAN station is shown by a white rectangle. (b) Comparison between the observed (thin line) and the synthetic apparent resistivity tensor ellipses (thick line). The synthetic ellipses are computed under the assumption that the best-fit conductance model (a in this figure) is given and that the source–receiver configuration is the same as the field experiment. Normalized uncertainty of the inversion parameter estimated for the best-fit model shown in (a) of this figure is also shown in the background. The maximum uncertainty is set to be 100%.

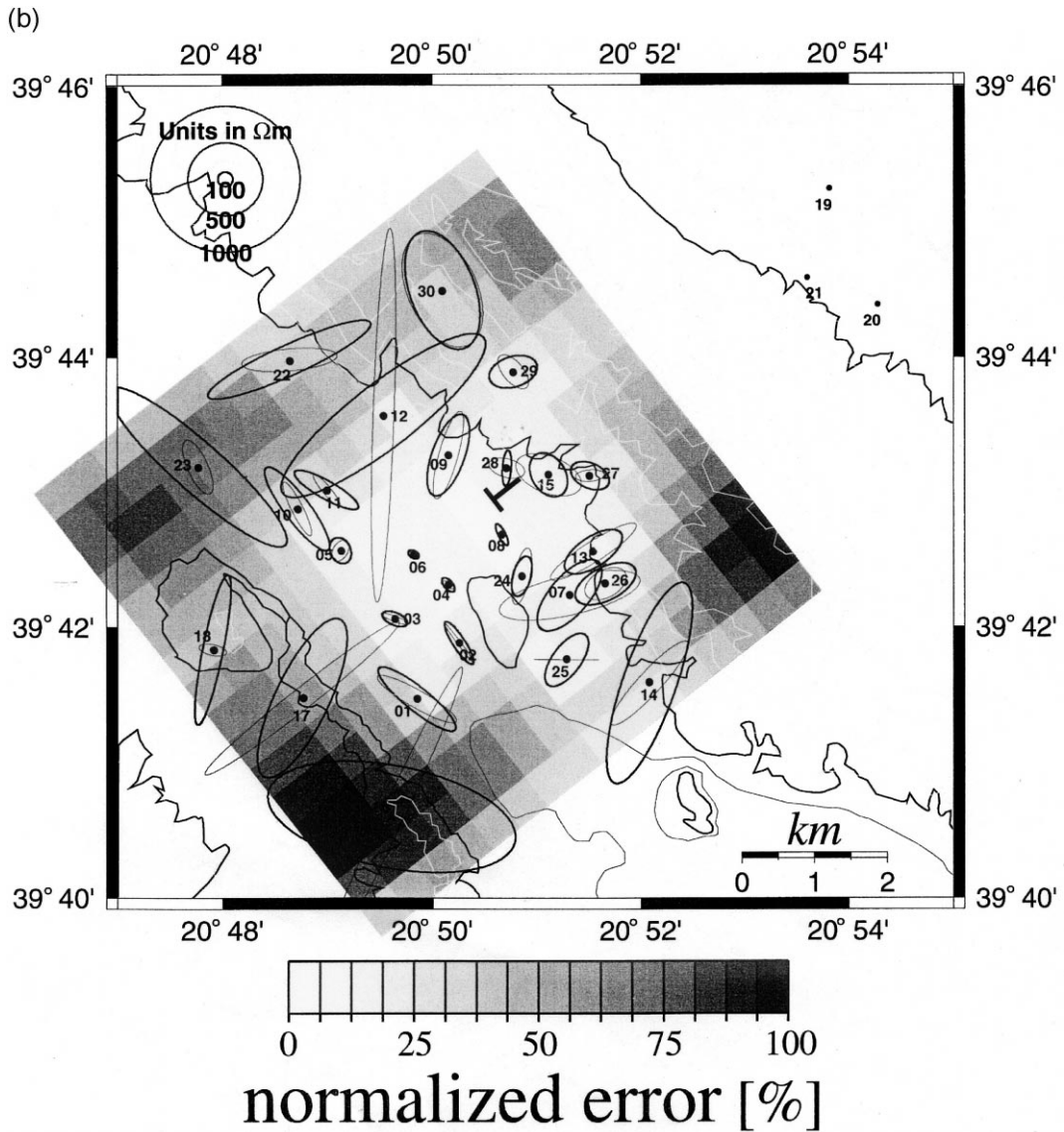


Fig. 6 (continued).

the background where the maximum uncertainty is set to be 100%. As a rough tendency, similar ellipses to those in Fig. 3(b) are estimated around the central part of the conductance map where the uncertainty is small because of rather dense receivers. On the other hand, some discrepancies are detected for the blocks with large uncertainty. The loci of the apparent resistivity tensors never take the form of circle, and are significantly influenced by the conductance con-

trast in the vicinity of receivers, as was mentioned in Section 3.

The inferred model shows nearly the same tendency as the apparent resistivity distribution shown in Fig. 3(a): features corresponding to resistive mountain and conductive basin are revealed again. Around IOA29 on the mountain and IOA18 on the limestone hill in the southeastern part of the area, relatively high conductance values are derived. The

conductance of IOA18 is probably not resolved by the inversion, since the apparent resistivity ellipse is not reproduced at all (Fig. 6(b)). The most conductive part in the basin is coincident with a negative peak of the gravity anomaly (Kono et al., 1996). The high conductance of the basin area may be caused by the low-density material, such as water in the sediment of the lake-bottom origin. However, around IOA10 towards IOA23 located in the basin, rather low conductances are obtained. In our modeling procedure used in this study, only the conductance value of the infinitesimally thin plate is obtained. Hence, the high conductance does not always correspond to the high conductivity. Just the product of the conductivity and the thickness of the plate can be obtained, so that a higher conductance corresponds also to a thicker conductive layer. This is probably the case concerning the conductance change of the basin in the study area. Judging from increase in conductance value from northwestern part of the basin where IOA23 is located towards the most conductive part around IOA06, the thickness of the conductive alluvium layer might increase. This feature is consistent with the gravity anomaly increasing northwestward. IOA13, closest to the VAN station is located on the resistive plate near the border between the conductive basin and the resistive mountain.

5. Electric field polarization around Ioannina VAN station

The apparent resistivity tensors were simulated when the current source was located at various places on the conductance distribution model shown in Fig. 6(a). The imaginary current sources were assumed to be orthogonal two dipoles of 96 m with 10 A current strength. Fig. 7(a) shows the polarization of the electric field at IOA13 due to a source at the ellipse location. A total of 100 ellipses at intervals of 480 m are shown together in the figure. If the computation area possesses uniform conductance distribution, all the resistivity tensor loci should be exact circles with the same radius. However, the actual resistivity tensor largely depends on the surrounding conductance distribution of the plate. If the source is located in the conductive part, the magnitude of the apparent resistivity gets small and vice versa. Even if the large source–receiver separation is assumed in the compu-

tation area, the extremely flattened ellipse is never obtained. The direction of the ellipses seems to be influenced by the most conductive part of the area.

The electric field polarization direction inferred from the MT recording of the ULF band (3–200 s) at the VAN station was ENE–WSW independent of direction of the magnetic field variation. The lightning electric field orientation was somewhat more scattered but still holds the same preferred direction as that of the MT electric field, which indicated the near-field effect (Uyeshima et al., 1998). The major axis direction of the ellipse as shown in Fig. 7(a) is completely different from the MT polarization. As far as the present model that assumes only the near-surface heterogeneity in the computation area is concerned, properties that were observed for the MT and lightning field could not be reproduced. It may be because the distance between the source and the receiver is still too short. The relationship between the source–receiver separation and the near-field range was studied for the controlled source audio-frequency magnetotellurics (CSAMT) by Zonge and Hughes (1987). They indicated that the data can be dealt as the near-field if the separation is smaller than the half of skin depth for all frequencies. In the case of our previous study, this near-field range limit can be calculated as about 7.5 km when we assume the average resistivity of 300 Ω m as shown in Fig. 3(a) and the shortest period of the recorded data (3 s, according to Uyeshima et al., 1998). The deviation of the electric field polarization of the lightning origin from the MT one was likely to be recorded at IOA station when the lightning stroke approached to around this near-field limit and/or when approached to more closer to the station though we did not have more deviated data of the lower period signals, which were filtered out. Our computation area shown in Fig. 7(a) is smaller than this near-field range, so that the current source position is local for the receiver and heterogeneous structure affects the polarization direction.

We made similar figures to Fig. 7(a) for other receivers. The location and the dimension of the current sources were assumed to be the same as in the case shown in Fig. 7(a). The elliptic representation of the resistivity tensors obtained at IOA01 is shown in Fig. 7(b). In this case, the ellipses get flattened pointing to nearly the same direction paral-

lel to the basin when the ellipse position (shown by an arrow in the figure) is located on the resistive side of the contact between the most conductive part (broken rectangle) and the northeastern resistive part. When the current source is placed just near the northeastern edge of the computation area, the polarization direction deviated from this trend and seemed

to be influenced by the conductance of plates near the receiver. As compared with Fig. 7(a), directions of ellipses are not the same despite the fact that they are located on the same plates close to the contact. This indicates that the conductance distribution around the source also affects the electric field polarization.

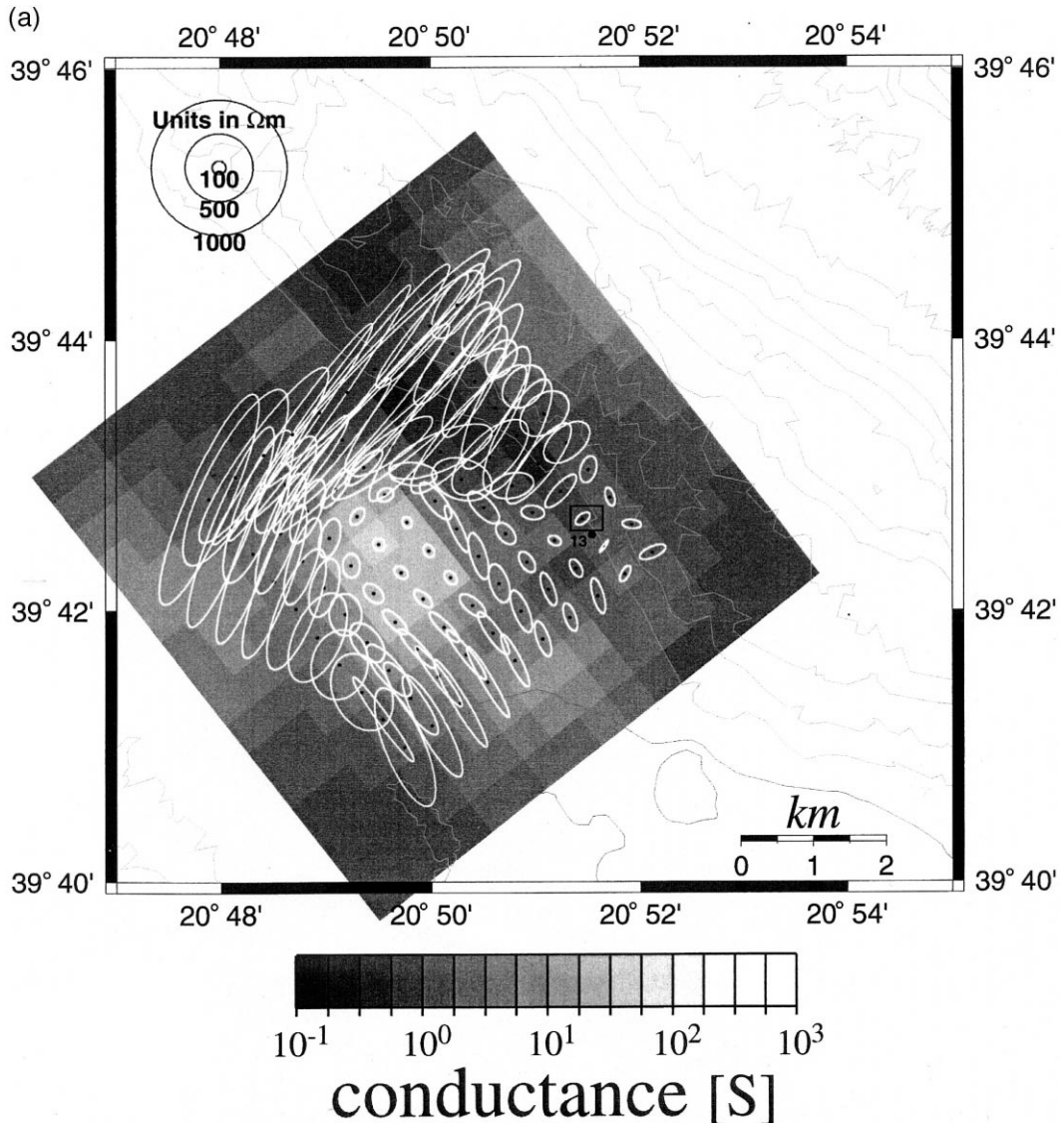


Fig. 7. (a) Elliptic representation of the apparent resistivity tensors expected at IOA13 when the current bipoles are put in the various places of the calculation area and the best-fit conductance model (Fig. 6(a)) is given. The VAN station is shown by a solid rectangle. (b) Elliptic representation of the apparent resistivity tensors expected at IOA01 when the current bipoles are put in the various places and the best-fit conductance model (Fig. 6(a)) is given. The VAN station is shown by a solid rectangle.

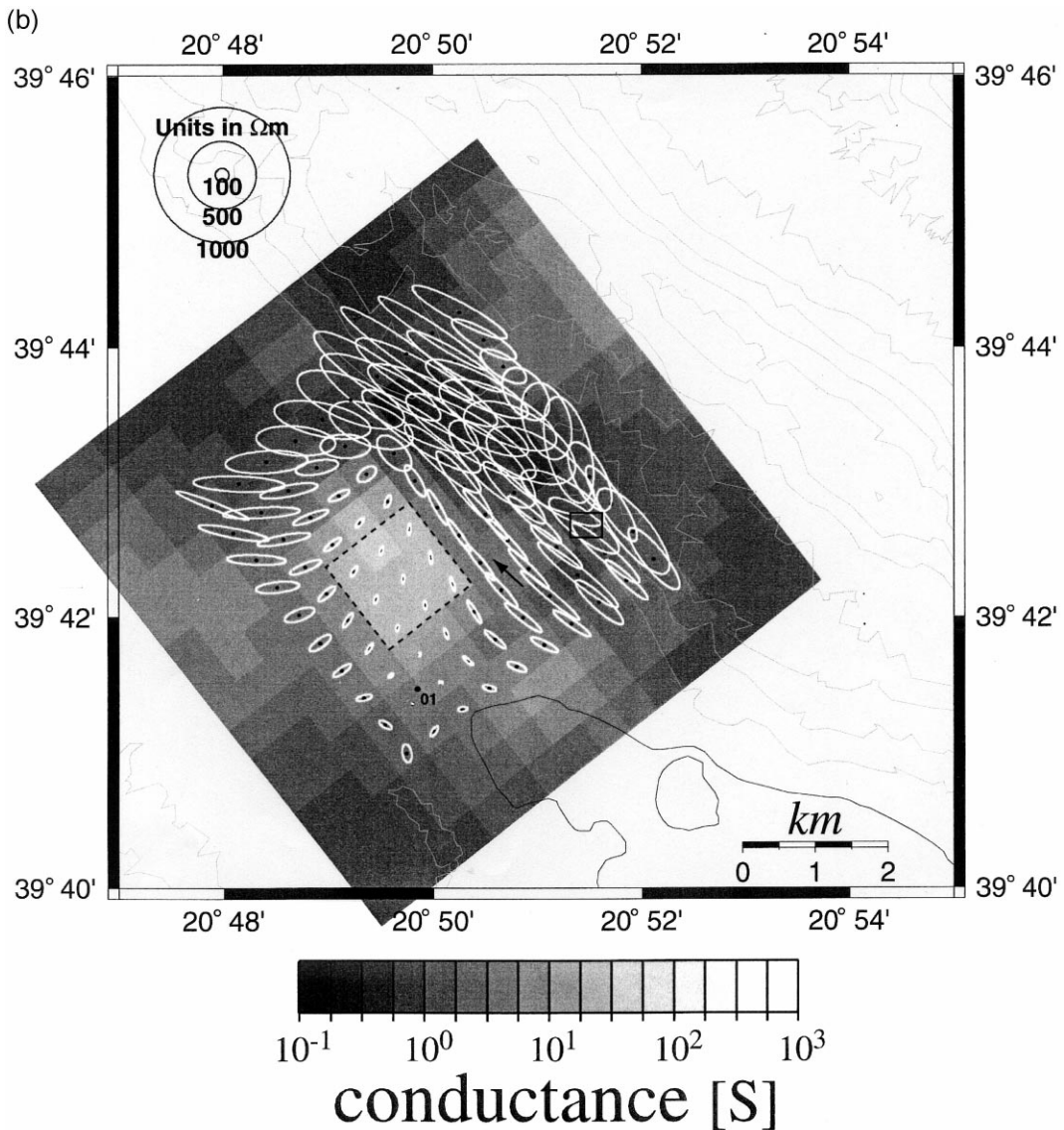


Fig. 7 (continued).

Some SES do not follow the same directional property as the MT field and their deviation from the MT preferred direction was more significant than that for nearby lightning electric field. The deviation is likely to be caused by the heterogeneous conductivity structure around the origin and the station. Thus, the origins of those SES are probably local in comparison with the EM induction scale length for

the Ioannina station. As seen in the simulated ellipses, the major axis direction seems to depend mainly on the location of the conductive part around the source. If we would like to seek the origin of the SES near the surface, it may be specified from the relationship between the location of the surrounding conductor and that of the VAN station. It is deduced that the further detailed mapping of the electrical

structure must be necessary by using the electromagnetic methods for this purpose.

6. Conclusion

We conducted a bipole–dipole survey around Ioannina VAN station in the summer of 1997. We succeeded in obtaining the data of high quality at a total of 30 receiver positions for two different bipole sources of the orthogonal directions. In this study, a model that expresses the electrical structure in terms of the surface heterogeneity of the conductance distribution was constructed by an inversion of the observed data. As a result, we found that the VAN station is located on the resistive side of the contact between the conductive basin and the resistive mountains.

The apparent resistivity tensor at IOA13 was simulated on the basis of the best-fit model with the imaginary source locations. We found that features of MT and lightning electric field at the VAN station were not reproduced. While the variation of the MT and lightning field possessed a clear polarized direction, the electric field polarization at IOA13, due to the current injection, was found to be significantly varied by the position of the source. These results suggest that the apparent resistivity tensors to be estimated depend on the resistivity distribution not only around receivers but also around the source.

Although more deviation from the polarized direction was detected as lightning stroke was nearer to the station, such a clear correlation was not reproduced for the electric field variation pattern due to the current injection as far as the source was located in the computation area. The source is considered to be local as compared to the scale of the surrounding electrical heterogeneity, which probably causes the large deviation. We may have the same directional property at IOA13 as the MT and lightning field polarization if the current source is placed at a larger distance out of the range in this study. To examine this hypothesis, we have to know the electrical structure in a wide range. Although the vertical information on the structure is included in the conductance distribution by the thin plate model in this study, we have to know the real three-dimensional structure and make a similar simulation under the assumption of the underground current source in the future study.

Acknowledgements

We are grateful to P. Varotsos and his group of the University of Athens for their kind cooperation in Greece; especially to K. Eftaxias, who made practical preparations for our survey. We also thank I. Suzuki and S. Kondo for their assistance in the fieldwork. Cu–CuSO₄ electrodes used in the fieldwork were made with the help by students of Tokai University under instruction by H. Murakami of Kochi University. We acknowledge Y. Makino of Kobe University for his advice on the data analysis. The constructive comments of S.K. Park and the anonymous reviewer are gratefully helpful to improve the manuscript. This study was conducted as a part of the 5-year research project “International Frontier Program on Earthquake Research” at the Institute of Physical and Chemical Research (RIKEN).

References

- Bibby, H.M., 1986. Analysis of multiple-source bipole–dipole resistivity surveys using the apparent resistivity tensor. *Geophysics* 51, 972–983.
- Groom, R.W., Bailey, R.C., 1989. Decomposition of impedance tensors in the presence of local three-dimensional galvanic distortions. *J. Geophys. Res.* 94, 1913–1925.
- Gruszow, S., Rossignol, J.C., Tzanis, A., Le Mouél, J.L., 1996. Identification and analysis of electromagnetic signals in Greece: the case of the Kozani earthquake VAN prediction. *Geophys. Res. Lett.* 23, 2025–2028.
- Hori, K., Kono, Y., Ogawa, T., Kanda, W., Uyeshima, M., Nagao, T., Takahashi, I., 1996. MT survey around VAN station in Ioannina, Greece. In: *Proceedings of 1996 Conductivity Anomaly Symposium*. pp. 143–156, (in Japanese).
- Kono, Y., Gennai, N., Yamaguchi, T., Hori, K., 1996. Gravity survey around VAN stations in Greece. In: *Report of Grant-in-Aid Scientific Research for International Scientific Research (cooperative study) (No. 06044085)*. Kono, Y. (Ed.), *Studies on the Greek-type Earthquake Prediction by using Self Potential Observation and its Application to Japan*. pp. 79–111, (in Japanese).
- Madden, T.R., 1972. Transmission systems and network analogies to geophysical forward and inverse problems, Rep. No. 72-3, Dept. of Geology and Geophysics, MIT, Cambridge, MA.
- Madden, T.R., Swift, C.M. Jr., 1969. Magnetotelluric studies of the electrical conductivity structure of the crust and upper mantle. Hart, P.J. (Ed.), *The Earth's Crust and Upper Mantle*. Am. Geophys. Union, *Geophys. Monogr.* 13, 469–479.
- Makris, J., Bogris, N., Eftaxias, K., 1997. Geoelectric structure of the VAN-station at Ioannina sensitive to the detection of

- seismic electric signals (SES). *Practica of the Athens Academy* 72, 1–119.
- Ogawa, T., Uyeshima, M., Kono, Y., Nagao, T., Hori, K., Takahashi, I., 1996. On the physical property of VAN's SES—comparison between SES and observed artificial electric field disturbances. In: *Proceedings of 1996 Conductivity Anomaly Symposium*. pp. 157–163, (in Japanese).
- Park, S.K., Fitterman, D.V., 1990. Sensitivity of the telluric monitoring array in Parkfield, California, to changes of resistivity. *J. Geophys. Res.* 95, 15557–15571.
- Uchida, T., 1993. Smooth 2-D inversion for magnetotelluric data based on statistical criterion ABIC. *J. Geomagn. Geoelectr.* 45, 841–858.
- Uyeshima, M., Kanda, W., Nagao, T., Kono, Y., 1998. Directional properties of VAN's SES and ULF MT signals at Ioannina, Greece. *Phys. Earth Planet. Inter.* 105, 153–166.
- Varotsos, P., Alexopoulos, K., 1984a. Physical properties of the variations of the electric field of the Earth preceding earthquakes, I. *Tectonophysics* 110, 73–98.
- Varotsos, P., Alexopoulos, K., 1984b. Physical properties of the variations of the electric field of the Earth preceding earthquakes: II. Determination of epicenter and magnitude. *Tectonophysics* 110, 99–125.
- Varotsos, P., Alexopoulos, K., 1986. Stimulated current emission in the earth: piezostimulated currents and related geophysical aspects. In: Amelinckx, S., Gevers, R., Nihoul, J. (Eds.), *Thermodynamics of Point Defects and their Relation with Bulk Properties*. North-Holland, Amsterdam, pp. 417–420.
- Varotsos, P., Alexopoulos, K., 1987. Physical properties of the variations of the electric field of the Earth preceding earthquakes, III. *Tectonophysics* 136, 335–339.
- Varotsos, P., Eftaxias, K., Lazaridou, M., Antonopoulos, G., Makris, J., Poliyiannakis, J., 1996a. Summary of the five principles suggested by Varotsos et al. [1996] and the additional questions raised in this debate. *Geophys. Res. Lett.* 23, 1449–1952.
- Varotsos, P., Lazaridou, M., Eftaxias, K., Antonopoulos, G., Makris, J., Kopanas, J., 1996b. Short term earthquake prediction in Greece seismic electric signals. In: Lighthill, J. (Ed.), *Critical Review on VAN: Earthquake Prediction From Seismic Electrical Signals*. World Sci. Publ., Singapore, pp. 29–76.
- Varotsos, P., Sarlis, N., Lazaridou, M., Kapiris, P., 1996c. A plausible model for the explanation of the selectivity effect of seismic electric signals. *Practica of the Athens Academy* 76, 283–353.
- Varotsos, P., Sarlis, N., Lazaridou, M., Kapiris, P., 1998. Transmission of stress induced electric signals in dielectric media. *J. Appl. Phys.* 83, 60–70.
- Zhang, J., Mackie, R.L., Madden, T.R., 1995. 3-D resistivity forward modeling and inversion using conjugate gradients. *Geophysics* 60, 1313–1325.
- Zonge, K.L., Hughes, L.J., 1987. Controlled source audio-frequency magnetotellurics. In: Nabighian, M.N. (Ed.), *Electromagnetic methods in applied Geophysics Vol. 2 SEG*, Tulsa, pp. 713–809, Part B.